JOURNAL OF GUIDANCE, CONTROL, AND DYNAMICS
Vol. 15, No. 2, March-April 1992

Active Damping by a Local Force Feedback with Piezoelectric Actuators

André Preumont,* Jean-Paul Dufour,† and Christian Malékian†
Free University of Brussels, Brussels B 1050, Belgium

This paper summarizes a research in the field of active damping of space structures. The test facility consists of a truss structure provided with two active elements that can be placed in various locations. Each of the active elements consists of a linear piezoelectric actuator collocated with a force transducer. Each active element is controlled in a decentralized manner, with an integral feedback of the force on the voltage applied to the piezoactuator. This control law is always stable and has been found very effective; the damping ratio of the first mode has been increased from 0.003 (open loop) to 0.09 with one actuator.

I. Introduction

LARGE space structures are subjected to a variety of dynamic perturbations produced by the crew, the docking of other spacecraft, transient thermal states during the orbit, micrometeorites, etc. The role of the damping is to limit the vibration amplitude and the settling time of the transients induced by these perturbations. In addition to that, the damping of the flexible modes is a necessary ingredient in achieving robust attitude control of the spacecraft, especially as the controller bandwidth and the flexible modes tend to overlap.[1]

Damping flexible structures can be achieved by passive (using viscoelastic materials) or active means. It is expected that the latter could achieve better performances with less weight. However, designing an active damping system is a challenging task because of the large number of modes involved in the bandwidth of interest and the large amount of uncertainty involved. In fact, the dynamic behavior of the spacecraft will hardly be known before launch, and the in-orbit identification will provide only limited information. This raises the question of robustness, for performance and especially for stability. This latter aspect was emphasized in the present study.

Piezoelectric actuators have recently attracted considerable interest[2-7] because they are wideband, simple, reliable, compact, and lightweight. Also, their power consumption is very small. However, they require a fairly high voltage (in the range of 500-1000 V), which may be a problem in the space environment (danger of an electrical arcing in the pressure range from 0.1 to 100 Torr). Heavy electronic support equipments are also needed.

There are two basic types of piezoelectric actuators, strips that are bonded on the structure, or linear actuators consisting of stacks of thin ceramic disks separated by electrodes. The former (sometimes called d_{31} to refer to the fact that the direction of expansion is normal to the direction of polarization and electrical field) can be used as distributed actuators for structures primarily subjected to bending deformations, whereas the latter (of the d_{33} type because the direction of expansion coincides with the direction of polarization) can be directly substituted to structural elements. By proper selection of the disks' sizes, the stiffness of the actuators can be tailored to a large extent. A mechanical preload is introduced to compensate for the small extensional strength of the stack.

As compared to previous works with linear actuators,[5-7] this study uses low-cost, commercially available actuators; the structure was tailored to the active element rather than the other way around.

The objectives of this project were set as follows:

1) Develop an active bar element consisting of a linear actuator collocated with a force transducer, using commercially available components. This active element essentially works like a muscle.

2) Substitute the active element in a truss structure and implement a digital control that is simple enough to fit into a PC/AT compatible, is robust enough to forgive large structural changes, and can be extended to provide a truly decentralized multidimensional control. This is motivated by the large model uncertainty mentioned before and the possibility of applying the control scheme to deployable structures. This approach is very much in contrast with Ref. 7, where the application of the optimal projection method required a very good model of the structure.

The control strategy adopted is a *local force feedback that provides a −90 deg phase shift between the piezoelectric extension and the measured force, in the appropriate bandwidth.* If this is obtained by an integrator, the control system can be made unconditionally stable, irrespective of the dynamics of the structure (at least in the continuous case without time delay or hysteresis in the actuator).

The efficiency of the control eventually relies on observability and controllability considerations that, in turn, can be reduced to a single index representing the *modal strain energy* distribution in the structure. This index can be used to select the number of actuators and their location.

II. Experimental Setup

The experimental setup is shown in Fig. 1. It consists of a vertical truss structure clamped at its base, with the active elements installed in its lower part, in the highest strain area. The natural frequencies are given in Table 1. The open-loop damping ratio of the first mode is 0.003. Because of the large frequency gap between modes 2 and 3, this study was focused on improving the damping of the first two modes.

The structure consists of a 12 bay truss of 14 cm length each, made of steel bars 4 mm in diameter. A mass of 2 kg is located at the top (that mass can be removed to check variations of the model). The joints consist of plastic balls in which the bars are glued.

The piezoelectric actuator is a Philips PXE HPA1, whose characteristics are summarized in Table 2. The reaction time is about 0.1 ms. The stroke-voltage characteristics are nonlinear and exhibit a rather high hysteresis.[8] The actuator operates between 0 and 500 V, with an average of about 250 V. The voltage source was originally developed at the University of Brussels but was later substituted by a power amplifier from

Received July 11, 1990; revision received Dec. 1, 1990; accepted for publication Dec. 5, 1990.

*Professor, Department of Applied Mechanics, CP165, 50, av. F. D. Roosevelt. Member AIAA.

†Assistant Professor, Department of Applied Mechanics, CP165, 50, av. F. D. Roosevelt.

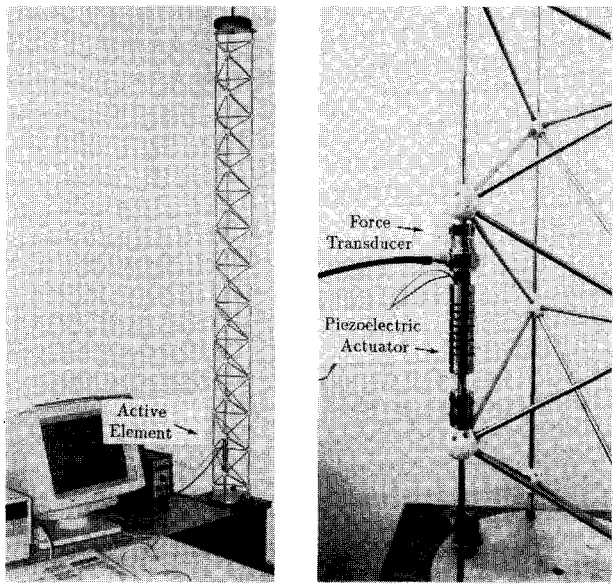

Fig. 1 Experimental setup and detail of the active element.

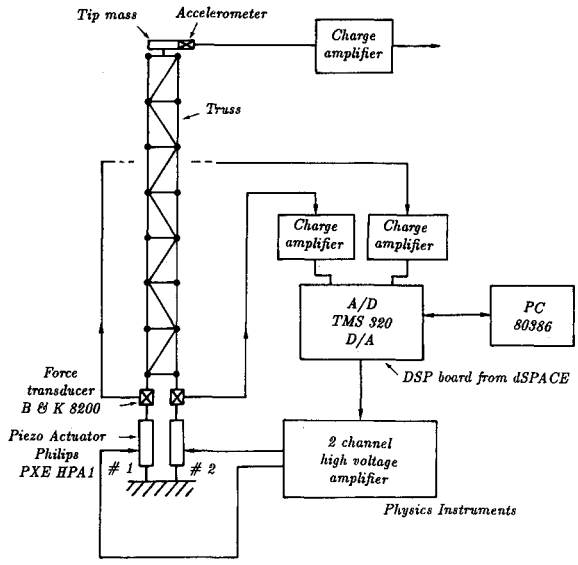

Fig. 2 Hardware configuration.

Table 1 Modal properties

Mode no.	Frequency, Hz	Mode shape
1	8.8	In-plane bending
2	10.5	Out-of-plane bending
3	58.1	Torsion
4	88.3	In-plane second mode

Table 2 Characteristics of the piezoelectric ceramic actuator

Diameter × length	16 × 50 mm
Stroke 0–500 V	20 μm
0–800 V	35 μm
Stiffness	30 N/μm
Maximum applied force	
Compression	2000 N
Extension	200 N

Physics Instruments. An interesting feature of the Philips actuator is the fact that the ceramic disks are pressed on each other rather than bonded as in other designs. This makes the actuator less sensitive to parasitic bending moments.

The force transducer is the standard Bruel & Kjaer 8200 with associated charge amplifier. It was originally connected to a PC/AT (80 286) compatible via an A/D converter. The sampling frequency of the control system was 200 Hz, which was enough to get good results. Later, a DSP processor was used, and the sampling rate could be increased to 1000 Hz. The final hardware configuration is represented in Fig. 2.

The overall stiffness of the active element approximately matches that of the bar it substitutes, so that the perturbation introduced by the active element is minimum.

For the purpose of this study, the actuator characteristics can be approximated by the relationship

$$\delta = Nd_{33}V \tag{1}$$

where δ is the axial extension, V is the applied voltage, N is the number of disks in the stack, and d_{33} is the piezoelectric constant. The exact relationship is nonlinear, $d_{33}(V)$, because of hysteresis.

III. Open Loop Transfer Function

The piezoelectric deformations are in all respects similar to thermal deformations. The equation of motion of an n degrees of freedom (DOF) undamped structure with m piezoelectric rods reads

$$M\ddot{x} + Kx = f + Bp \tag{2}$$

where x and f are the n vectors of nodal displacements and forces, B is the $n \times m$ matrix of directional cosines of the active elements, and p is the m vector of equivalent piezoelectric forces, whose components are related to the piezoelectric extensions δ by

$$p = K_a\delta \tag{3}$$

where $K_a = \text{diag}(E_iA_i/L_i)$ is the stiffness of the active elements, and δ is approximately proportional to the applied voltage as in Eq. (1).

The measured force is proportional to the elastic deformation of the active elements

$$y = K_a(B^Tx - \delta) \tag{4}$$

where B^Tx represents the total relative displacements of the nodes of the active members. The same matrix B appears in Eqs. (2) and (4) because the actuators and sensors are collocated.

From Eq. (2) to Eq. (4), the open loop frequency response is obtained as

$$y = K_a[B^T(K - \omega^2M)^{-1}BK_a - 1]\delta \tag{5}$$

Upon substituting the spectral expansion of the dynamic flexibility matrix,

$$(K - \omega^2M)^{-1} = \sum_{i=1}^{n} \frac{\phi_i\phi_i^T}{\mu_i(\Omega_i^2 - \omega^2)} \tag{6}$$

where ϕ_i are the mode shapes, and Ω_i the natural frequencies, one gets

$$y = K_a\left[\sum_{i=1}^{n} \frac{B^T\phi_i\phi_i^TBK_a}{\mu_i(\Omega_i^2 - \omega^2)} - 1\right]\delta \tag{7}$$

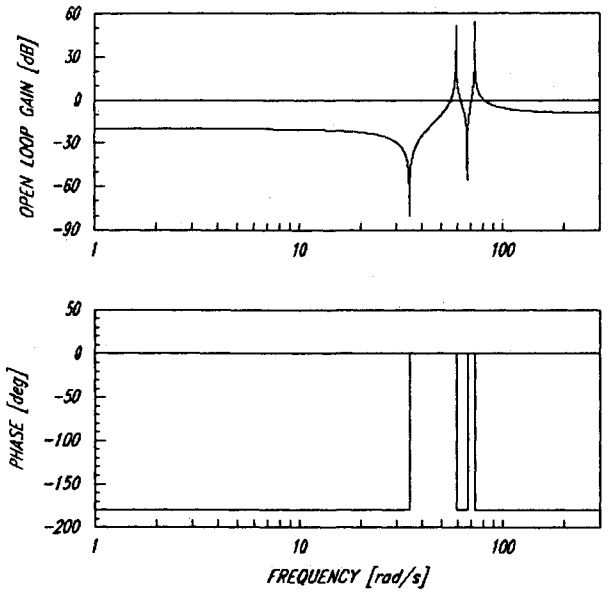

Fig. 3 Open-loop frequency response function $G(\omega)$.

In the single-input/single-output case, introducing the fraction of modal strain energy in the active element

$$\nu_i = \frac{\phi_i^T B K_a B^T \phi_i}{\mu_i \Omega_i^2} = \frac{\phi_i^T B K_a B^T \phi_i}{\phi_i^T K \phi_i} \tag{8}$$

the open-loop frequency response reads

$$y = K_a G(\omega)\delta \tag{9}$$

with

$$G(\omega) = \sum_{i=1}^{n} \frac{\nu_i}{1 - (\omega/\Omega_i)^2} - 1 \tag{10}$$

One observes that there is a feedthrough component and the residue of each complex pole of $G(\omega)$ is equal to ν_i, the fraction of strain energy in the active element, for the corresponding mode shape. *It can be regarded as a compound index of controllability and observability.*

A typical plot of $G(\omega)$ is shown in Fig. 3 with a model including 2 modes (a finite frequency resolution provides some artificial damping near the poles and zeros). One observes a typical feature of systems with collocated actuators and sensors: the poles and zeros occur by pairs. Note that the finite element results obtained with beam and bar elements are very close.

IV. Control Law

The control law consists of a force feedback

$$\delta = -H(j\omega)y \tag{11}$$

where the output filter is chosen to provide a -90 deg phase shift between the piezoelectric extension and the measured force, in the frequency band of interest (the first two modes in this case). Two candidates were investigated:

Differentiator (plus low pass filter):

$$H(j\omega) = \frac{j\omega g}{K_a} \cdot F(j\omega) \tag{12}$$

Integrator:

$$H(j\omega) = \frac{-g}{j\omega K_a} \tag{13}$$

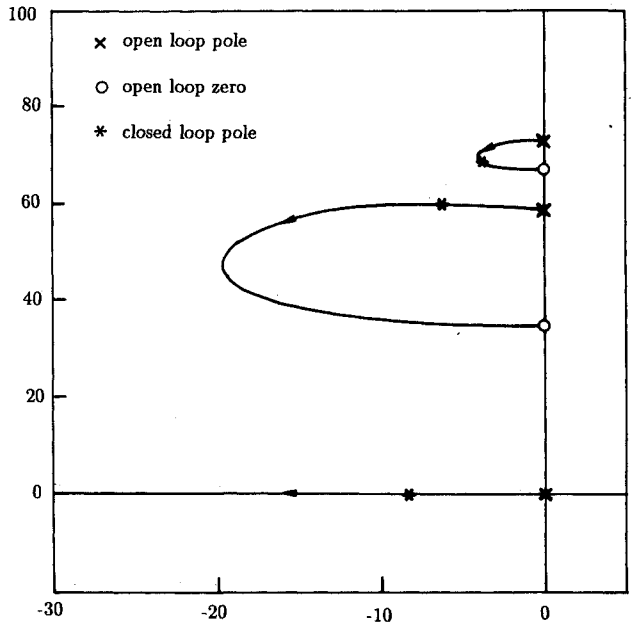

Fig. 4 Typical root locus plot of the closed-loop system, $\nu_1 = 0.12$, $\nu_2 = 0.12$.

It turns out that the differentiator is conditionally stable and that the stability condition depends on the low pass filter used. For a first-order filter $[F(j\omega) = (a + j\omega)^{-1}]$, the stability condition is $ga < 1$. Some experimental results obtained with this control law are reported in Ref. 8. On the contrary, the integral control in Eq. (13) is always stable. A typical root locus plot for the closed loop system is shown in Fig. 4; the closed-loop poles move from the poles to the zeros of the open-loop system. The exact shape of the plot depends on the parameters ν_i that control the spacing between the poles and the zeros as well as the size of the loop connecting them (and therefore the damping). This root locus plot resembles that of the attitude control of a flexible satellite with collocated actuator and sensor (e.g., see Ref. 9). We shall focus on the integral control in the sequel of this paper because it is unconditionally stable and it has been found extremely efficient. In addition to the positive aspects stated earlier, the integral control is extremely simple to implement digitally:

$$\delta_{i+1} = \delta_i + g\Delta t y_{i+1}$$

On the other hand, one must be careful to avoid the classical problem of saturation. This can be achieved by slightly modifying the previous relationship according to

$$\delta_{i+1} = \alpha\delta_i + g\Delta t y_{i+1}$$

where the forgetting factor $\alpha < 1$ can be tuned experimentally. This amounts to shifting the pole at the origin of Fig. 4 slightly to the left along the real axis. It is readily checked that this does not significantly affect the loci of the flexible poles.

Note that the conclusions about the stability of the integral control have been reached in the ideal, continuous case, with no time delay or hysteresis, etc. In practice, however, this control scheme has been found extremely robust, even at high gains.

V. Modal Damping

Combining Eqs. (4), (11), and (13), one gets the feedback relationship between the piezoelectric extension and the structural displacement

$$\delta = -\frac{jg}{\omega - jg} B^T x = \frac{jg(\omega + jg)}{\omega^2 + g^2} B^T x \tag{14}$$

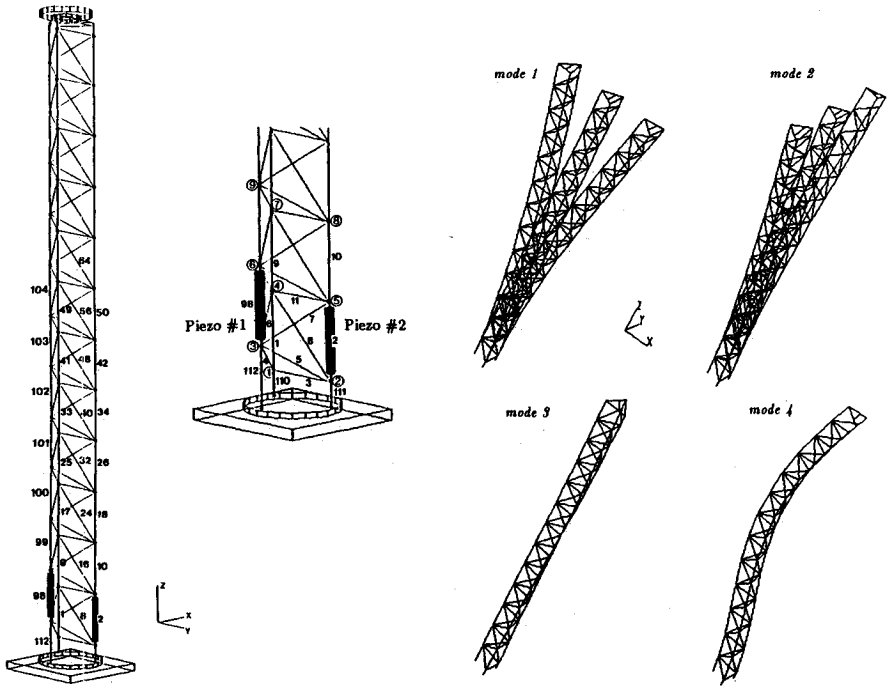

Fig. 5 Finite element model and mode shapes (results obtained with beam and bar elements are very close).

Table 3 Fraction of strain energy in selected elements (numbering according to Fig. 5)

w_i	1.0	1.0	1.0	0	
f_i, Hz	8.8	10.5	58.1	88.3	$\Sigma \nu_i w_i$
98	15.7	0.1	0.6	7.4	16.4
1	4.1	11.2	0.1	3.6	15.4
2	3.1	11.4	0.1	2.1	14.7
9	3.4	9.4	0.1	1.3	12.8
10	2.6	9.4	0.2	0.8	12.2
112	11.6	0.0	0.5	10.9	12.1
99	10.6	0.0	0.3	1.3	11.0
17	2.8	7.7	0.1	0.2	10.5
18	2.1	7.6	0.3	0.1	10.0
100	8.6	0.0	0.2	0.0	8.8
25	2.2	6.2	0.1	0.1	8.5
26	1.7	6.0	0.4	0.0	8.1
101	6.7	0.0	0.1	1.4	6.8
33	1.7	4.8	0.1	0.7	6.6
34	1.3	4.6	0.5	0.4	6.3
102	5.1	0.0	0.1	4.1	5.2
41	1.3	3.6	0.1	1.5	5.0
42	1.0	3.4	0.5	1.0	4.9

Upon Fourier transforming Eq. (2) and substituting Eqs. (3) and (14), one gets the closed-loop dynamic flexibility matrix:

$$x = \left[-\omega^2 M + j\omega \frac{g}{\omega^2 + g^2} BK_a B^T + K - \frac{g^2}{\omega^2 + g^2} BK_a B^T \right]^{-1} f \tag{15}$$

The $j\omega$ term can be interpreted as a damping matrix. One observes that, thanks to the collocation of the actuator and sensor, BK_aB^T is semi-positive definite. This guarantees that all observable and controllable modes will be damped (at least in the continuous case with no delay and no actuator and sensor dynamics involved). If one transforms into modal coordinates

$$x = \Phi z \tag{16}$$

one easily gets

$$\left[-\omega^2 \mu + \mu\Omega^2 \left(j\omega \frac{g}{\omega^2 + g^2} \nu + 1 - \frac{g^2}{\omega^2 + g^2} \nu \right) \right] z = \Phi^T f \tag{17}$$

with the usual matrix notations

$$\mu = \text{diag}(\mu_i) = \Phi^T M \Phi \tag{18a}$$

$$\mu\Omega^2 = \text{diag}(\mu_i \Omega_i^2) = \Phi^T K \Phi \tag{18b}$$

$$\nu = (\Phi^T K \Phi)^{-1} (\Phi^T B K_a B^T \Phi) \tag{19}$$

This matrix is, in general, not diagonal. Its diagonal terms are the fractions of modal strain energy in the active element given by Eq. (8). If one neglects the off-diagonal components of ν, Eq. (17) can be reduced to a set of uncoupled equations:

$$\mu_i \Omega_i^2 \left[-\frac{\omega^2}{\Omega_i^2} + j \frac{\omega}{\Omega_i} \left(\frac{g \Omega_i \nu_i}{\omega^2 + g^2} \right) + 1 - \frac{g^2}{\omega^2 + g^2} \nu_i \right] z = \phi_i^T f \tag{20}$$

For small gains ($g \ll \Omega_i$), the active damping ratio is approximately

$$\xi_i = \frac{g \nu_i}{2\Omega_i} \tag{21}$$

Thus, *the active damping ratio in a given mode is proportional to the fraction of modal strain energy in the active element for that mode.* It is also observed that, with the integral control, the active damping ratio decreases as the natural frequency increases.

VI. Actuator Location

More than any specific control law [Eq. (11)], the stiffness and the location of the active element are likely to be the most important factors affecting the control system performances. The active elements should be located where their authority over the modes to control is the largest. The result of Sec. V is quite appealing because it links the modal damping to the fraction of strain energy in the active element, which constitutes a compound index for observability and controllability. Thus, the search for candidate locations where active elements

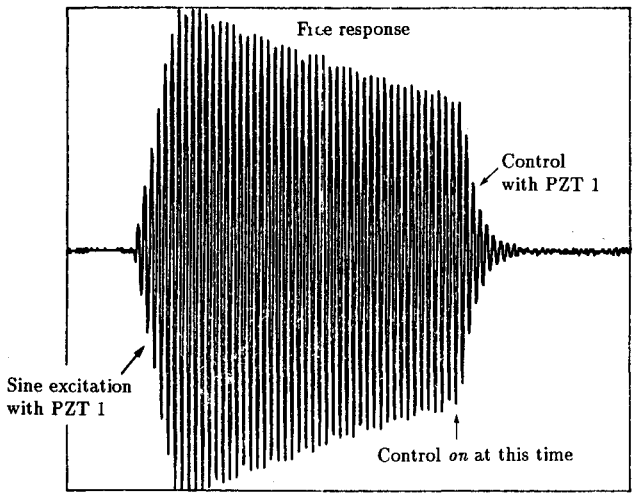

Fig. 6 Force signal from PZT 1; sine excitation, free response, followed by active damping.

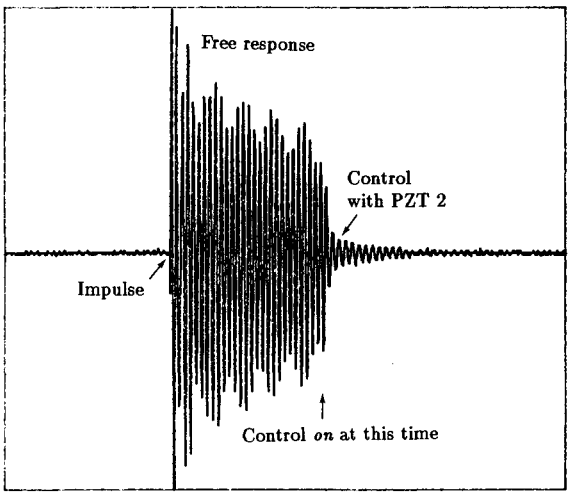

Fig. 8 Force signal from PZT 2; free response followed by active damping.

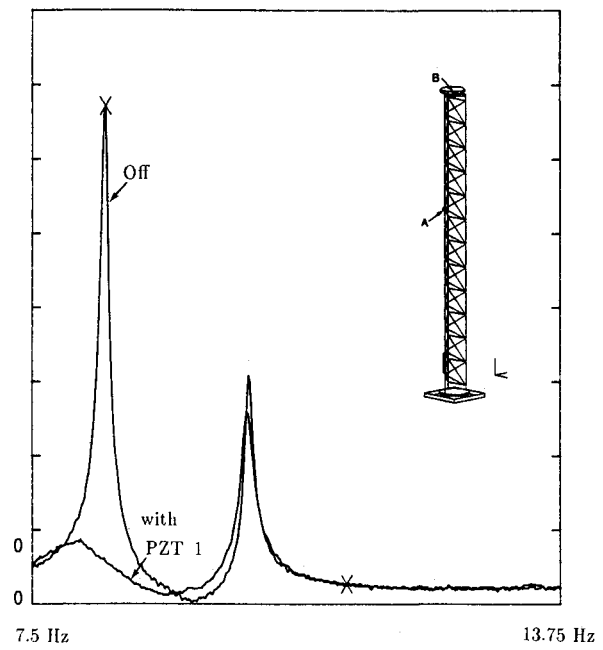

Fig. 7 Frequency response function between A and B, with and without control of PZT 1 in element 98.

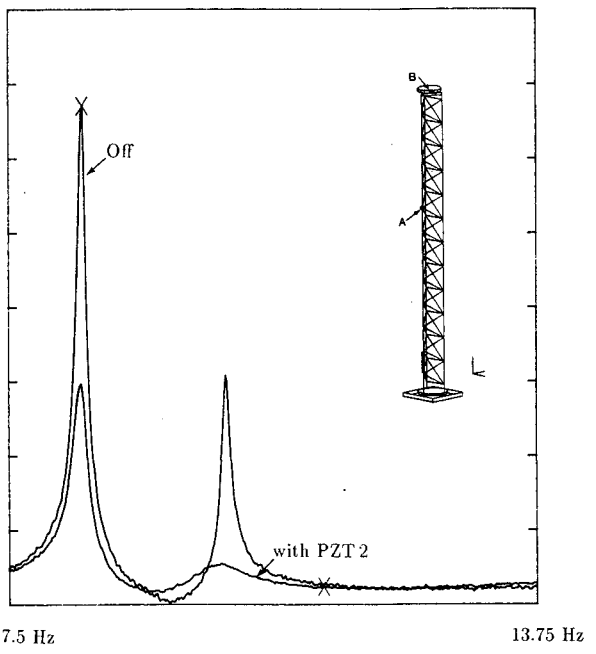

Fig. 9 Frequency response function between A and B, with and without control of PZT 2 in element 2.

can be substituted is greatly assisted by the examination of the map of fraction of strain energy in the structural elements, which is directly available in commercial finite-element packages. Such a map is presented in Fig. 5 and Table 3; the mode shapes are also shown in Fig. 5. From the table, one observes that substituting the active member to element no. 98 provides a strong control of mode 1 (in-plane bending mode) but no control of mode 2 (out-of-plane bending), which is almost not observable or controllable. Table 3 can be used in two ways:

1) The various modes can be given weights w_i (e.g., related to the performance requirements), and the active elements are substituted at locations that maximize $\sum \nu_i w_i$ (this information is given in the last column of Table 3, with equal weights for the first three modes).

2) The locations can be chosen on the ground that they offer the capability of controlling a large number of modes (e.g., elements 1 or 2 to control the first two modes). This can be achieved by minimizing $\sum w_i/\nu_i$.

VII. Experimental Results

Figure 6 shows the force signal sensed by the active member located in element 98 of the model during the following sequence of events: starting from rest, a sine voltage, at a frequency close to the first natural frequency of the structure, is applied to the actuator and then stopped. The free response is observed. After a while, the control is turned on, and the closed-loop response is recorded. It can be seen that the decay rate of the first mode (the only observable from this location) is increased substantially.

For the same location of the active member, Fig. 7 shows the frequency response functions (average over two tests), with and without control, between the acceleration at the top (B) and the force applied at A, both at an angle of about 45 deg (so as to have a contribution from the first two modes). One observes that the peak of the first mode is considerably attenuated by the control system, whereas the second mode remains almost unaffected. This is because it is neither observ-

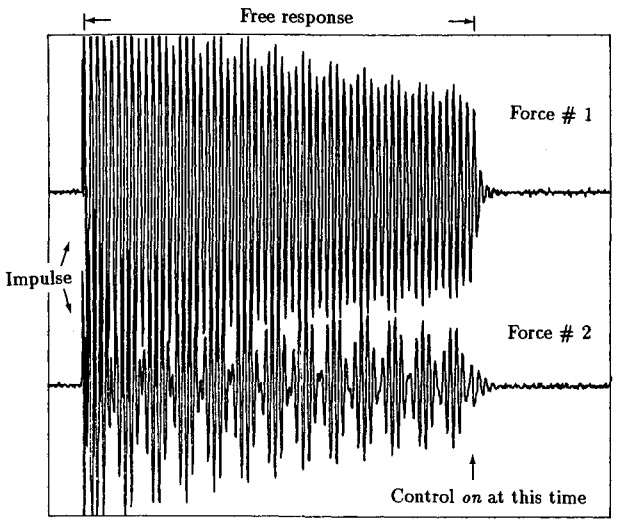

Fig. 10 Decentralized control; force signal from PZT 1 and PZT 2 and free response followed by active damping.

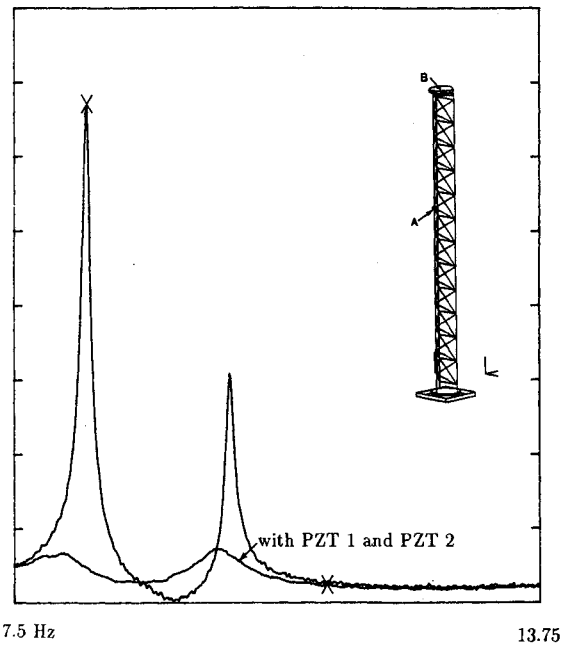

Fig. 11 Decentralized control of PZT 1 and PZT 2; frequency response function between A and B, with and without control.

able nor controllable by the active member in the present location (see the first line of Table 3).

In Fig. 8, the active member is located in element 2 of the model (Fig. 5). The figure shows the force signal after the structure has been hit with an instrumented hammer. Here again, the open- and closed-loop responses are compared. In this case, one can observe the beating that results from the interaction between the first two modes.

Figure 9 is similar to Fig. 7 for that new location. One observes that mode 2 is considerably attenuated while some damping is also provided to mode 1. This agrees with the third line of Table 3.

Finally, decentralized control has been implemented using two active members located in elements 98 and 2, respectively. Figure 10 shows the force signal after the structure has been hit impulsively. Again, the open- and closed-loop responses are compared. Once again, force signal 1 is dominated by the first mode, while the beating is observed in force signal 2. Figure 11 shows the frequency response functions when both active elements are in operation. As expected, both modes are significantly reduced.

The damping ratio depends on the gain and the number of active elements in operation. It has been possible to increase the damping ratio of the first mode to 0.09 with one actuator. A damping ratio larger than 0.10 has been obtained with two actuators.

In Fig. 8, it is interesting to note that the noise level after the transient has been settled is comparable to that before the control is turned on.

VIII. Conclusion

A low-cost active member has been developed using commercially available components. It consists of a piezoelectric linear actuator collocated with a force transducer. A decentralized control based on local integral force feedback has been implemented digitally, using two active members located in the appropriate manner in a truss structure. The control law has very good stability properties and is very effective. The damping ratio of the first mode has been increased from 0.003 to 0.09 with one actuator and to more than 0.10 with two actuators. The simplicity, performance, and robustness of the control methodology may be attractive for future large space structures.

References

[1]Hughes, P. C., and Abdel-Rahman, T. M., "Stability of Proportional-Plus Derivative-Plus Integral Control of Flexible Spacecraft," *Journal of Guidance and Control,* Vol. 2, No. 6, 1979, pp. 499–503.

[2]Fanson, J. L., and Caughey, T. K., "Positive Position Feedback Control for Large Space Structures," *AIAA Journal,* Vol. 28, No. 4, 1990, pp. 717–724.

[3]Crawley, E. F., and de Luis, J., "Use of Piezoelectric Actuators as Elements of Intelligent Structures," *AIAA Journal,* Vol. 25, No. 10, 1987, pp. 1373–1385.

[4]Burke, S. E., and Hubbard, J. E., "Active Vibration Control of a Simply Supported Beam Using a Spatially Distributed Actuator," *IEEE Control System Magazine,* Aug. 1987, pp. 25–30.

[5]Fanson, J. L., Blackwood, C. H., and Chu, C. C., "Active Member Control of a Precision Structure," *Proceedings of the 30th AIAA/ASME/ASCE/AHS Structures, Structural Dynamics, and Materials Conference,* AIAA, Washington, DC, 1989, pp. 1480–1494.

[6]Chen, G. S., Lurie, B. J., and Wada, B. K., "Experimental Studies of Adaptive Structure for Precision Performance," *Proceedings of the 30th AIAA/ASME/ASCE/AHS Structures, Structural Dynamics, and Materials Conference,* AIAA, Washington, DC, 1989, pp. 1462–1472.

[7]Peterson, L. D., Allen, J. J., Lauffer, J. P., and Miller, A. K., "An Experimental and Analytical Synthesis of Controlled Structural Design," *Proceedings of the 30th AIAA/ASME/ASCE/AHS Structures, Structural Dynamics, and Materials Conference,* AIAA, Washington, DC, 1989, pp. 91–103.

[8]Preumont, A., Sparavier, M., and Dufour, J. P., "Application of Piezoelectric Actuators to the Active Damping of a Truss Structure," *Proceedings of the 31st AIAA/ASME/ASCE/AHS Structures, Structural Dynamics, and Materials Conference,* AIAA, Washington, DC, 1990, pp. 1907–1913.

[9]Franklin, G., Powell, J. D., and Emami-Naeini, A., *Feedback Control of Dynamic Systems,* Addison-Wesley, Reading, MA, 1986.